

## Article

# Rheological Properties of Ultra-Fine Tailings Cemented Paste Backfill under Ultrasonic Wave Action

Weicheng Ren <sup>1,2</sup> , Rugao Gao <sup>3,\*</sup>, Youzhi Zhang <sup>1,2</sup> and Maoxin Hou <sup>1,2</sup>

<sup>1</sup> School of Mining Engineering, North China University of Science and Technology, No. 21, Bohai Road, Tangshan 063009, China; kygcxy4137@ncst.edu.cn (W.R.); zhangyouzhi@ncst.edu.cn (Y.Z.); jxzy@ncst.edu.cn (M.H.)

<sup>2</sup> Key Laboratory of Mining and Safety Technology of Hebei Province, North China University of Science and Technology, No. 21, Bohai Road, Tangshan 063009, China

<sup>3</sup> College of Resources and Safety Engineering, Central South University, No. 932, Lushan Road (South), Changsha 410083, China

\* Correspondence: gaorgcsu@csu.edu.cn; Tel.: +86-15874290401

**Abstract:** Ultra-fine tailings cemented paste backfill (UCPB) exhibits special rheological characteristics with the effect of an ultrasonic sound field. In this study, in order to explore the thickening effect of slurry under ultrasonic wave action, we examined the rheological properties with ultrasonic wave tests of UCPB and the rheological properties after ultrasonic wave tests of UCPB. We found that the rheological curve of the slurry changed; the Herschel–Bulkley (HB) model in the initial state transformed into the Bingham model under the action of ultrasound. Ultrasonic waves have a positive effect on reducing slurry viscosity and yield stress. The rheological test of the slurry with ultrasonic wave action had a positive effect on significantly reducing the apparent viscosity and initial yield stress of slurry with a 62% mass concentration. The rheological test of slurry with ultrasonic wave action and the rheological test after ultrasonic wave action both have positive effects on reducing the viscosity and yield stress of the slurry with a 64% to 68% mass concentration; the overall effect of reducing the viscosity and yield stress of UCPB is greater after ultrasonic wave action of UCPB.

**Keywords:** ultra-fine tailings cemented backfill (UCPB); rheological properties; ultrasonic waves; slurry pipeline transportation



**Citation:** Ren, W.; Gao, R.; Zhang, Y.; Hou, M. Rheological Properties of Ultra-Fine Tailings Cemented Paste Backfill under Ultrasonic Wave Action. *Minerals* **2021**, *11*, 718. <https://doi.org/10.3390/min11070718>

Academic Editor: Abbas Taheri

Received: 9 June 2021

Accepted: 2 July 2021

Published: 3 July 2021

**Publisher's Note:** MDPI stays neutral with regard to jurisdictional claims in published maps and institutional affiliations.



**Copyright:** © 2021 by the authors. Licensee MDPI, Basel, Switzerland. This article is an open access article distributed under the terms and conditions of the Creative Commons Attribution (CC BY) license (<https://creativecommons.org/licenses/by/4.0/>).

## 1. Introduction

The rheological characteristics of mortar in the process of conveying slurry is one of the important parameters for judging fluidity, which directly affects the stability of the tailing silo, pipe conveying, and other links [1–3]. However, the rheological problems of slurry, such as the ease of solidifying the tailings discharge at the mouth of the tailing silo and the ease of blocking the conveyor pipe, are often perplexing for mining enterprises in high-concentration tailings cemented filling [4–6] and seriously affect filling efficiency and cost. Therefore, it is important to study how to effectively improve the rheological properties of slurry for continuous mine filling operations [7–9].

In recent years, studies have been conducted to investigate the factors that influence the rheological properties of backfilling slurry from different aspects [10–12]. Ali et al. found that the addition of silicate and sodium silicate could improve the rheological properties of mortar [13,14]. Roshani et al. found that the yield stress and viscosity of slurry containing nanocrystalline silica increased significantly at different temperatures [15]. Xue et al. found that a high temperature environment and the addition of fly ash reduced the yield stress of slurry and enhanced the rheological properties of slurry [16]. Taheri et al. analyzed the effects of different types and dosages of gels on the rheological properties of slurry [17]. Fall et al. found that yield stress showed a trend of decline as the initial sulphate

concentration was increased, while the apparent viscosity showed the opposite trend [18]. Zhang et al. used fly ash powder (FA), ground slag (GGBS), and quicklime as mineral admixtures and analyzed the rheological properties of foam-cemented backfill [19]. Guo et al. analyzed the effect of an efficient water reducer on the rheological properties of superfine tailings cemented paste through the theory of water film thickness [20]. Majid et al. analyzed the effects of slurry concentration, additives, cement content, temperature, pH value, particle size distribution, and other factors on rheological parameters [21]. Lima et al. used recycled fine aggregate from building waste as an additive to study its effect on the rheology of cement slurry [22]. It is not difficult to see that the above studies were mainly based on the influence of additives, slurry concentration, temperature, pH, and other factors on the rheological properties of slurry. However, some admixtures pollute mine environments and affect the early or long-term strength of backfill, and therefore, the cost of slurry preparation is higher [23–25].

As a type of sound wave, ultrasonic waves have the advantages of strong penetration and good directivity. Relevant studies have used ultrasonic wave action to improve the rheological properties of slurry such as sludge, coal water slurry, and cement tailing mortar, and have achieved good effects [26–29]. Ultrasonic wave action effectively reduces the use of admixtures, saves economic costs, and also improves the ecological environment to a certain extent. Zhao et al. studied the effect of ultrasound on the dewatering of biological sludge in sewage treatment plants under different conditions [30]. Ruiz-Hernando et al. examined changes in the rheological features of secondary sludge as a function of ultrasonic specific energy [31]. Luo et al. analyzed the mechanism of ultrasonic degradation of oily sludge and found that low-frequency ultrasound could generate larger and stronger cavitation bubbles, which were more effective in oil desorption [32]. Zhu et al. found that ultrasonic wave action could significantly improve the rheological properties of filling slurry and reduce the plastic viscosity and yield stress of total tailings slurry [33,34]. However, the effect of ultrasound on the rheological properties of UCPB has not attracted the attention of researchers, and there are few studies on the mechanism of UCPB.

In this study, rheological tests of slurry with and after ultrasonic wave action were carried out using a rheological tester and homemade ultrasonic container. In this study, we analyzed the effect of ultrasonic wave action on the rheological properties of slurry in order to provide a reference for its application in the mine filling process.

## 2. Methods and Materials

### 2.1. Materials

Tailings were collected from an iron mine processing plant in Hebei Province, China. The physical and chemical properties of the tailings were tested by the Tangshan Institute of Geology and Mineral Bureau of Hebei Province. The chemical composition of the tailings is listed in Table 1, indicating that the main chemical components of the tailings are SiO<sub>2</sub>, Al<sub>2</sub>O<sub>3</sub>, total iron as oxides, MgO, and CaO, which amount to 90.52% of the total weight. The physical properties of the tailings are provided in Table 2. The tailings were free of sulfide minerals. The particle size distribution of the tailings is shown in Figure 1.

Portland cement was chosen as the cementitious materials. A mixture of UCPB, water, and cement was used as the test sample.

**Table 1.** Chemical composition of used tailings.

Composition	SiO <sub>2</sub>	Al <sub>2</sub> O <sub>3</sub>	Total Iron	MgO	CaO	Loss on Ignition
Content (%)	67.24	7.30	6.00	5.60	4.04	9.48

**Table 2.** Physical parameters of used tailings.

Density (g·cm <sup>-3</sup> )	Average Particle Size (μm)	Porosity (%)	Specific Surface Area of Volume (cm <sup>2</sup> ·cm <sup>-3</sup> )
2.620	15.05	40.99	11457.6

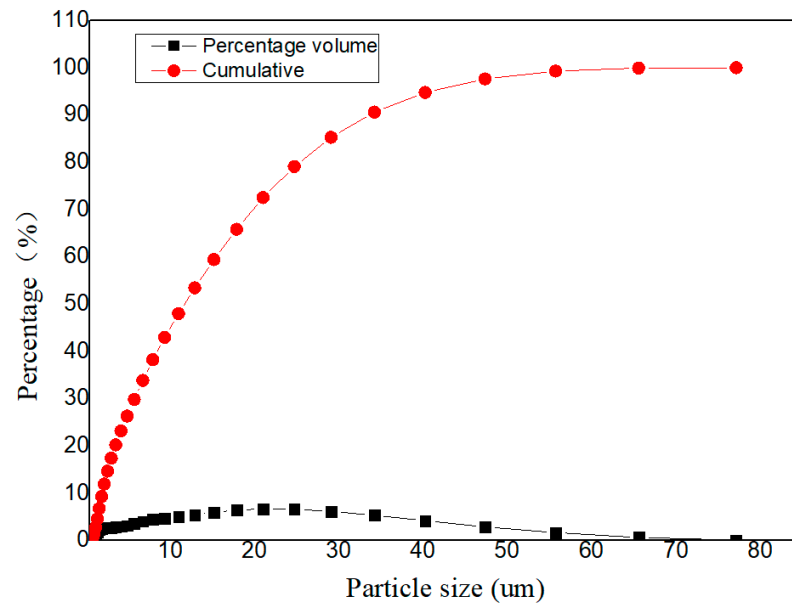


Figure 1. The particle size distribution of the tailings.

2.2. Preparation of UCPB Mixtures

The UCPB samples were prepared with a cement/tailing (c/t) ratio of 1:4, and the specimens had a mass concentration of 62–70% by weight, which is commonly used in the Hebei Iron mine. The details of the mixtures are listed in Table 3.

Table 3. The UCPB mix proportions for rheological tests.

Mixture Volume (m <sup>3</sup> )	Cement/Tailing Ratio	Solid Content (%)	Cement (kg)	Ultra-Fine Tailings (kg)	Water (kg)
0.0002	1:4	62	0.041	0.163	0.125
		64	0.043	0.172	0.121
		66	0.045	0.181	0.116
		68	0.048	0.190	0.112

The filling slurry with a 62% mass concentration was segregated, and it was considered to be a low-concentration slurry; the filling slurry did not have obvious segregation when the mass concentrations were 64%, 66%, and 68%, thus, these were considered to be high-concentration slurries [35–38]. The slurry segregation state is shown in Figure 2.



Figure 2. Slurry segregation state.

### 2.3. Testing and Monitoring of Samples

To obtain the rheological parameters of UCPB, the rheological tests, rheological properties under ultrasonic wave action, and rheological properties after ultrasonic wave action were conducted as follows:

#### 2.3.1. Rheological Tests of UCPB

A rheometer (HAAKE Viscotester iQ, Thermo Fisher Scientific, Waltham, MA, USA) was used to test the rheological behavior of the UCPB. The test was started with a controlled shear rate (CR) process, and a computer monitoring system was used to capture data samples (shear rate, shear stress, and apparent viscosity) every second. The shear rate sweep was set to a CR increase from 0 to 100 r/s for 60 s.

#### 2.3.2. Rheological Tests of UCPB under Ultrasonic Wave Action

As shown in Figure 3, the experimental equipment for rheological testing consisted of the following: (1) an ultrasonic container, (2) a rheometer, (3) a container with the mixture, and (4) a rotor. The bottom of the slurry container was equipped with an ultrasonic generator and converter, and the radiation effect of ultrasonic waves from the bottom to top optimized the fluidity of the slurry. The HAAKE Viscotester iQ rheometer was used and the ultrasonic container was customized through Mojie Ultrasonic Equipment Co., Ltd. (Guangzhou, China). A model FL22 rotor (Thermo Fisher Scientific, Waltham, MA, USA) was selected. The test was carried out immediately after the preparation of the slurry. The ultrasonic radiation was performed simultaneously with the rotation of the rotor of the rheometer. Ultrasonic waves were applied to the slurry when the rheometer started to work. The shear rate sweep was set to a CR increase from 0 to 100 r/s for 60 s. The ultrasonic wave was set to a frequency of 28 kHz and a power of 12 W.

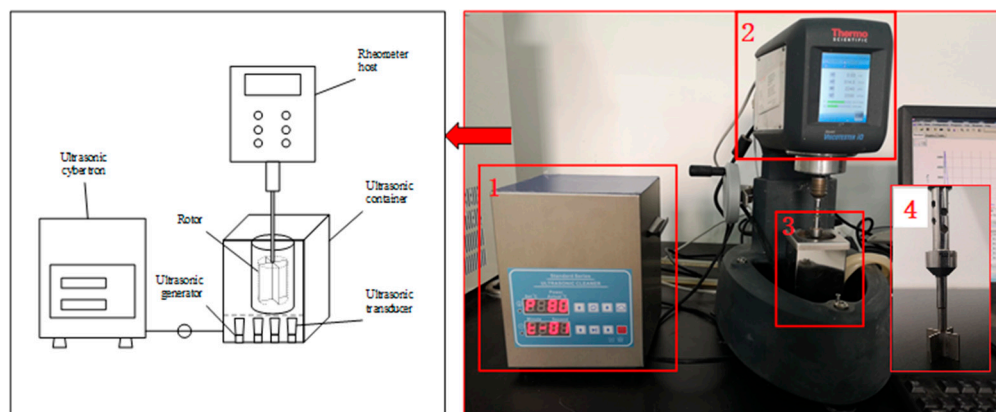


**Figure 3.** Rheometer and ultrasonic container.

#### 2.3.3. Rheological Tests of UCPB after Ultrasonic Wave Action

This experiment consisted of two steps, i.e., the slurry was subjected to ultrasonic radiation, and then rheological tests. In the first step, the UCPB was subjected to ultrasonic action for 60 s, and the ultrasonic wave was set to a frequency of 28 kHz and power of 12 W. In the second step, the rheological tests were carried out, and the shear rate sweep was set to a CR increase from 0 to 100 r/s for 60 s.

## 3. Results and Discussion

### 3.1. The Rheological Behavior of UCPB

The shear rate and the shear stress were automatically recorded by the rheometer apparatus. The apparent shear stress vs. shear rate flow curves of the UCPB mixtures are

presented in Figure 4. The experimental studies showed that the rheological behavior of UCPB mixtures may be sufficiently described by the Hershel–Bulkley equation as follows:

$$\tau = \tau_0 + \mu\dot{\gamma}^n \quad (1)$$

where  $\tau$  (Pa) is the shear stress;  $\dot{\gamma}$  (1/s) is the shear rate,  $n$  is the Hershel–Bulkley (H-B) index; and  $\tau_0$  (Pa) and  $\mu$  (Pa·s) are the initial yield shear stress and plastic viscosity, respectively. The values of the shear stress and shear rate were substituted into the HB model, and Table 4 illustrates the results of fitting Equation (1). It is worth noting that the higher the slurry concentration, the more consistent the curve form is with the HB model [39].

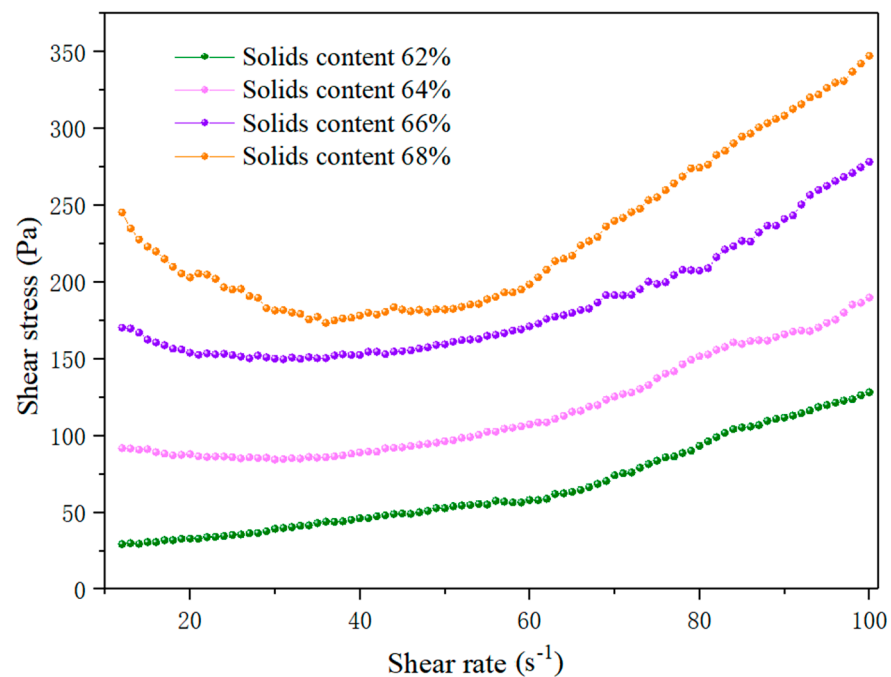


Figure 4. Shear rate versus shear stress flow curves of UCPB.

Table 4. Fitting equation parameters of UCPB.

Solid Content (%)	Apparent Viscosity (Pa·s)	Initial Yield Shear Stress (Pa)	Index $n$	R (%)
62	1.11	31.55	2.31	99.2
64	1.79	83.04	2.75	98.3
66	2.63	152.61	3.71	98.6
68	3.32	188.79	3.92	90.3

The effect of concentration on the viscosity and yield stress of filling slurry is obvious. The viscosity value and yield stress value of tailing slurry increases gradually with an increase in concentration. A change in the free water content of the slurry causes a change in the dispersion degree of structural units in the slurry, and then affects the viscosity value of the filling slurry macroscopically. The free water quantity decreases with an increase in the concentration of the filling slurry, and the dispersion degree of structural units decreases when the cement/sand ratio of the filling slurry remains constant. Therefore, the viscosity value of the slurry increases. However, the free water in the slurry is in a state of supersaturation in a certain range of low slurry concentrations and has no obvious effect on the dispersion effect of the structural units.

### 3.2. The Rheological Behavior of UCPB with Ultrasonic Wave Action

Slurry rheological tests with ultrasonic effects were carried out using a rheometer and homemade ultrasonic container. The apparent shear stress vs. shear rate flow curves of UCPB mixtures with ultrasonic wave action are presented in Figure 5. The curves of shear rate and shear stress of filling slurry changed with the ultrasonic wave action. The experimental studies show that the rheological behavior of UCPB mixtures with ultrasonic wave action may be sufficiently described by the Hershel–Bulkley equation.

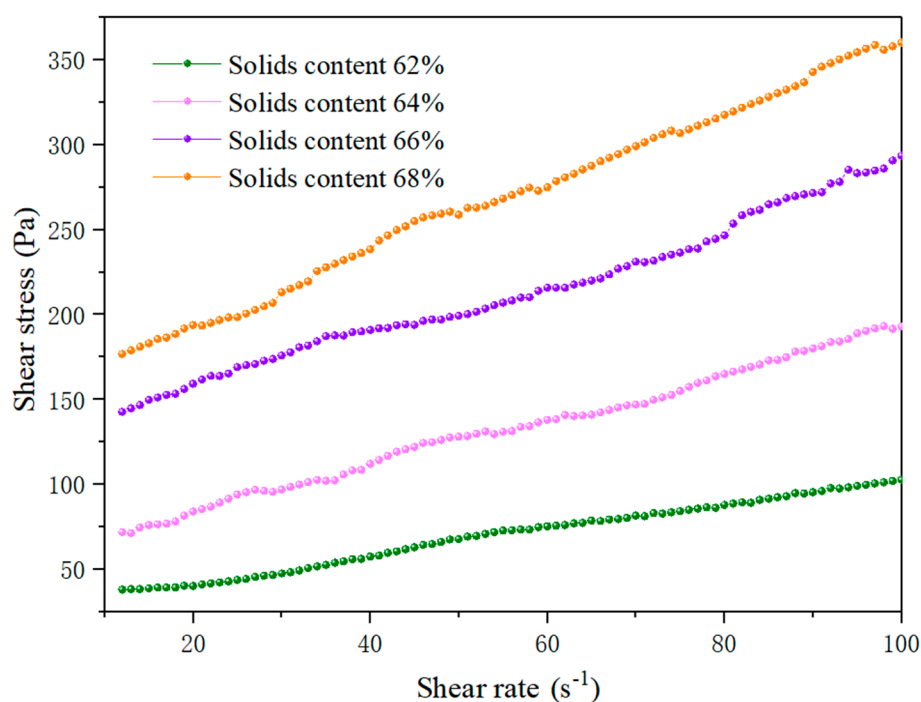


Figure 5. Shear rate versus shear stress flow curves of UCPB with ultrasonic wave action.

The values of the shear stress and shear rate were substituted into the HB model, and Table 5 illustrates the results of fitting Equation (1).

Table 5. Fitting equation parameters of UCPB with ultrasonic wave action.

Solid Content (%)	Apparent Viscosity (Pa·s)	Initial Yield Shear Stress (Pa)	Index $n$	R (%)
62	0.85	20.45	1.12	97.7
64	1.33	55.38	1.09	98.5
66	1.66	142.02	1.15	97.2
68	1.99	157.83	1.11	98.1

Viscosity and yield stress still changed regularly with mass concentration, i.e., the higher the concentration, the greater the viscosity and yield stress. The slurry absorbs the ultrasonic energy when the ultrasonic wave propagates in the slurry. It intensifies the vibration of molecules in the equilibrium position, increases the energy of molecular chains, and at the same time enhances the activity of molecular chains. Thus, it weakens the interaction between molecular chains and reduces the viscous resistance to flow. As the degree of freedom and energy of the single molecular chain increase, the conformation of the molecular chain of the filling slurry changes under the action of ultrasound. At the same time, the thermal effect caused by the ultrasonic cavitation produces high temperature and high pressure in an instant. It still produces thermal degradation of the surrounding molecular chains, although the scope of action is small [40,41]. The microjet and shock

waves shear part of the molecules and decrease the molecular weight of the filling slurry. The change in molecular structure resulted in a decrease in the viscosity of filling slurry.

### 3.3. The Rheological Behavior at UCPB after Ultrasonic Wave Action

Slurry rheological tests after ultrasonic effects were carried out using a rheometer and homemade ultrasonic container. The apparent shear stress vs. shear rate flow curves of UCPB mixtures after ultrasonic waves are presented in Figure 6. The filling slurries with mass concentrations of 62%, 64%, 66%, and 68% conform to the HB model. The filling slurry with a 62% mass concentration is considered to be a low-concentration filling slurry. It is easy to destroy the molecular arrangement structure in the slurry after the ultrasonic action is completed, when the rotor rotates. Therefore, the curve form is the same as that of the filling slurry without the ultrasonic effect. The filling slurries with mass concentrations of 64%, 66%, and 68% are considered to be high-concentration slurries. It is difficult for the rotor to destroy the molecular arrangement structure after ultrasonic treatment in a short time, because of the high viscosity of the slurry. Therefore, the curve form is the same as that of the filling slurry accompanied by ultrasonic wave action. Table 6 shows the fitting results of Equation (1).

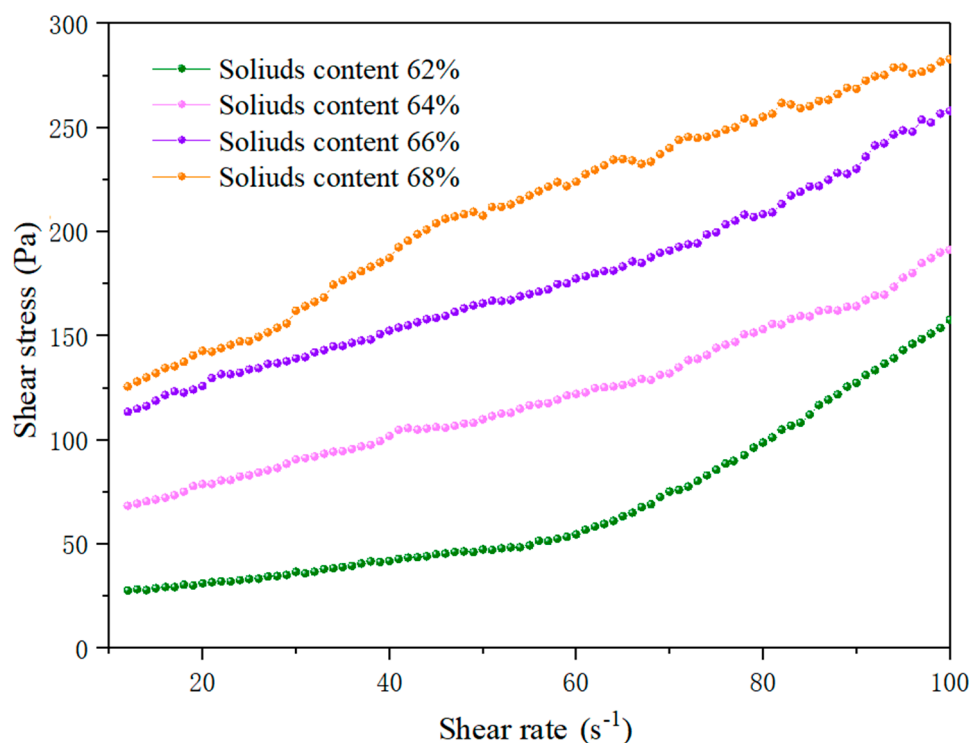


Figure 6. Shear rate versus shear stress flow curves of UCPB after ultrasonic wave action.

Table 6. Fitting equation parameters of UCPB after ultrasonic wave action.

Solid Content (%)	Apparent Viscosity (Pa·s)	Initial Yield Shear Stress (Pa)	Index <i>n</i>	R (%)
62	1.03	31.15	3.04	98.3
64	1.17	52.59	1.14	97.5
66	1.41	125.88	1.12	98.1
68	1.92	148.74	0.97	98.5

### 3.4. Effects of Ultrasonic Wave Action on the Yield Stress and Viscosity of UCPB

In order to further explore the influence of ultrasonic wave action on the rheological properties of UCPB, the yield stress and viscosity of the filling slurries with mass concentrations of 62%, 64%, 66%, and 68% were compared and analyzed. Table 7 shows the rheological tests results for the apparent viscosity and initial yield shear stress of filling slurries, obtained (a) without ultrasonic wave action of UCPB, (b) with ultrasonic wave action of UCPB, and (c) after ultrasonic wave action of UCPB. The apparent viscosity vs. mass concentration curves of UCPB are presented in Figure 7. The initial yield shear vs. mass concentration curves of UCPB are presented in Figure 8.

**Table 7.** Apparent viscosity and initial yield shear stress of filling slurry.

Mass Concentration (%)	Without Ultrasonic Waves of UCPB		With Ultrasonic Waves of UCPB		After Ultrasonic Waves of UCPB	
	Apparent Viscosity (Pa·s)	Initial Yield Shear Stress (Pa)	Apparent Viscosity (Pa·s)	Initial Yield Shear Stress (Pa)	Apparent Viscosity (Pa·s)	Initial Yield Shear Stress (Pa)
62	1.11	31.55	0.85	20.45	1.03	31.15
64	1.79	83.04	1.33	55.38	1.17	52.59
66	2.63	152.61	1.66	142.02	1.41	125.88
68	3.32	188.79	1.99	157.83	1.92	148.74

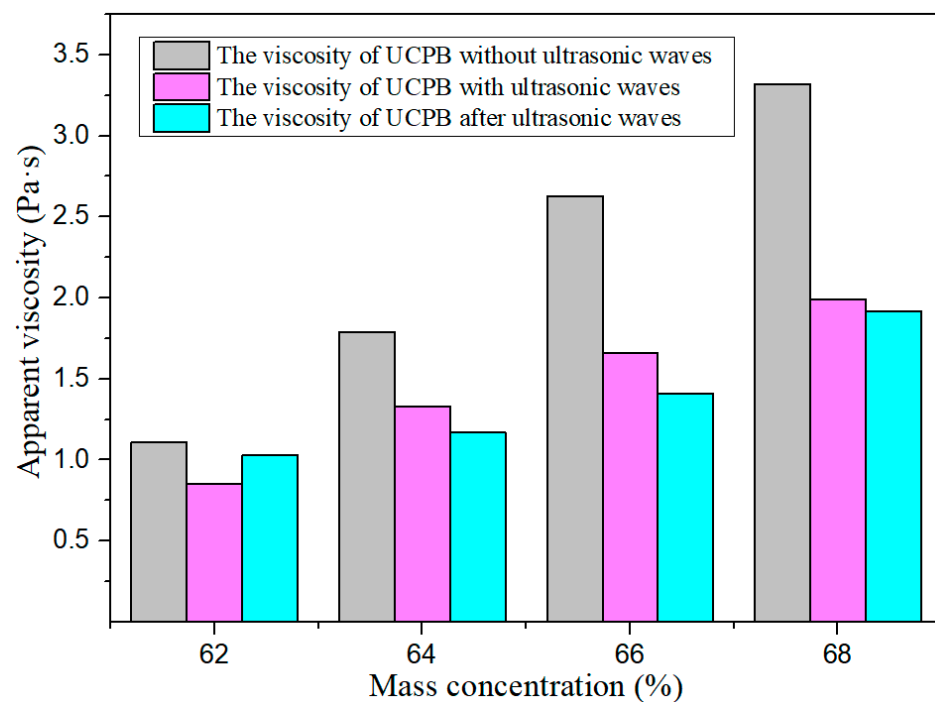


**Figure 7.** Apparent viscosity vs. mass concentration curves of UCPB.

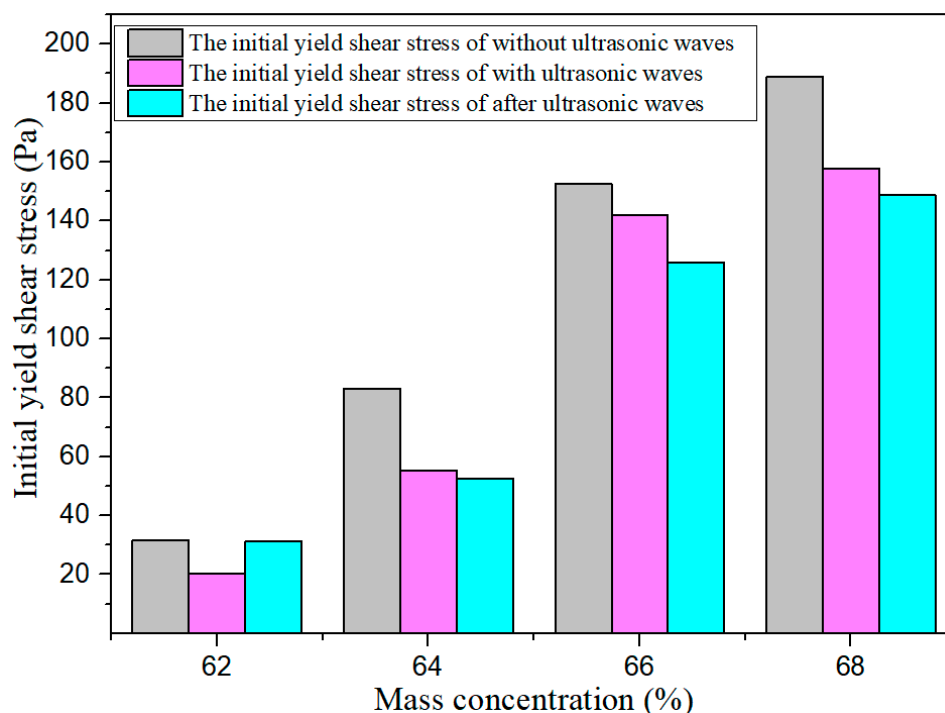


**Figure 8.** Initial yield shear vs. mass concentration curves of UCPB.

The velocity of ultrasonic waves varies in different media, and the velocity differences produce shear force and directional force at the interface between the water and tailings. Directional force can cause strong mechanical vibrations of medium particles centered on their equilibrium positions. The shear force can weaken the binding force between the medium, so that the viscosity and yield stress are reduced.

The higher the slurry concentration, the higher the viscosity and the higher the initial shear stress. The viscosity and initial stress of different concentrations are decreased with and after ultrasonic action. The results showed that the ultrasonic wave had different effects on the molecular arrangement of slurry. The effect of filling slurry with ultrasonic waves on reducing the apparent viscosity and initial stress of slurry is better when the mass concentration of filling slurry is 62% as compared with conventional technology, i.e., the apparent viscosity is reduced by 23% and the initial stress is reduced by 35%. The effect of filling slurry after ultrasonic wave action on reducing the apparent viscosity and initial stress of slurry is better when the mass concentration of the filling slurry is above 64% as compared with conventional technology, i.e., the apparent viscosity is reduced by 42% and the initial stress is reduced by 21%.

#### 4. Conclusions

In this study, the rheological properties of filling slurry with mass concentrations of 62%, 64%, 66%, and 68% were studied under three conditions, i.e., no ultrasonic action, with ultrasonic action, and after ultrasonic action. The rheological curve, viscosity, and initial stress were compared and analyzed.

The following conclusions can be drawn based on the above results:

- (1) The effect of concentration on the viscosity and yield stress of filling slurry is obvious. Ultrasonic wave action has a positive effect on reducing slurry apparent viscosity and initial yield shear stress. The effects of UCPB with and after ultrasonic wave action on reducing the apparent viscosity and initial stress of slurry are both better if the UCPB is of high concentration.
- (2) Ultrasonic effects on slurry in different time periods also have different effects on its fluidity. It is worth noting that the effect on UCPB with ultrasonic wave action on reducing the apparent viscosity and initial stress of slurry is better if the UCPB

is of low concentration. However, the overall effect of reducing the viscosity and yield stress of UCPB is more significant after ultrasonic wave action of UCPB, and the higher the slurry concentration, the better the effect.

- (3) The rheological test of slurry with ultrasonic wave action has a positive effect on reducing the viscosity and yield stress of slurry with a 62% mass concentration, in which the apparent viscosity is reduced by 23% and the initial yield shear stress is reduced by 35%. The rheological test of slurry with ultrasonic action and the rheological test after ultrasonic action both have good effects on reducing the viscosity and yield stress of the slurries with a 64% to 68% mass concentration, however, the overall effect of reducing the viscosity and yield stress of UCPB is more outstanding after ultrasonic wave action of UCPB, i.e., the apparent viscosity is reduced by 42% and the initial stress is reduced by 21%.

**Author Contributions:** Writing—original draft preparation, W.R.; Writing—review and editing, R.G.; data processing, Y.Z. and M.H. All authors have read and agreed to the published version of the manuscript.

**Funding:** This research was supported by the Natural Science Foundation of Hebei Province, China (no. E2020209041) the Basic Scientific Research Operating Expenses of Provincial Universities in Hebei Province (no. JQN2019002), and the Science and Technology Project of Tangshan City (no. 20130207b).

**Data Availability Statement:** All data derived from this research are presented in the enclosed figures and tables.

**Conflicts of Interest:** The authors declare no conflict of interest.

## References

1. Qiu, J.P.; Guo, Z.B.; Yang, L. Effects of packing density and water film thickness on the fluidity behaviour of cemented paste backfill. *Powder Technol.* **2019**, *359*, 27–35. [[CrossRef](#)]
2. Brito, G.; Jerez, O.; Gutierrez, L. Incorporation of Rheological Characterization in Grinding and Tailings Slurries to Optimize the CMP Magnetic Separation Plant. *Miner* **2021**, *11*, 386. [[CrossRef](#)]
3. Zhou, K.P.; Gao, R.G.; Gao, F. Particle flow characteristics and transportation optimization of superfine unclassified backfilling. *Miner* **2017**, *7*, 6. [[CrossRef](#)]
4. Chen, Q.S.; Zhang, Q.L.; Fourie, A. Experimental investigation on the strength characteristics of cement paste backfill in a similar stope model and its mechanism. *Constr. Build. Mater.* **2017**, *154*, 34–43. [[CrossRef](#)]
5. Ouattara, D.; Belem, T.; Mbonimpa, M. Effect of superplasticizers on the consistency and unconfined compressive strength of cemented paste backfills. *Constr. Build. Mater.* **2018**, *181*, 59–72. [[CrossRef](#)]
6. Ren, W.C.; Gao, R.G.; Gan, D.Q. Model of Consecutive, Steady-State Underflow for Vertical Tailing Silos. *Adv. Mater. Sci. Eng.* **2019**, *2019*, 2980548. [[CrossRef](#)]
7. Mbonimpa, M.; Kwizera, P.; Belem, T. Mine Backfilling in the Permafrost, Part II: Effect of Declining Curing Temperature on the Short-Term Unconfined Compressive Strength of Cemented Paste Backfills. *Minerals* **2019**, *9*, 172. [[CrossRef](#)]
8. Dalce, J.B.; Li, L.; Yang, P.Y. Experimental Study of Uniaxial Compressive Strength (UCS) Distribution of Hydraulic Backfill Associated with Segregation. *Minerals* **2019**, *9*, 147. [[CrossRef](#)]
9. Yang, L.; Xu, W.; Yilmaz, E.; Wang, Q.; Qiu, J. A combined experimental and numerical study on the triaxial and dynamic compression behavior of cemented tailings backfill. *Eng. Struct.* **2020**, *219*, 110957. [[CrossRef](#)]
10. Ren, W.C.; Wang, S.F.; Gao, R.G. Operational process simulation and optimization of a continuous-discharge system in a backfilling system. *Mater. Tehnol.* **2019**, *53*, 101–107. [[CrossRef](#)]
11. Saedi, A.; Jamshidi-Zanjani, A.; Darban, A.K. A review on different methods of activating tailings to improve their cementitious property as cemented paste and reusability. *J. Environ. Manage.* **2020**, *270*, 110881. [[CrossRef](#)] [[PubMed](#)]
12. Yilmaz, T.; Ercikdi, B.; Devenci, H. Utilisation of construction and demolition waste as cemented paste backfill material for underground mine openings. *J. Environ. Manage.* **2018**, *222*, 250–259. [[CrossRef](#)] [[PubMed](#)]
13. Ali, G.; Fall, M.; Alainachi, I. Time- and Temperature-Dependence of Rheological Properties of Cemented Tailings Backfill with Sodium Silicate. *J. Mater. Civil Eng.* **2021**, *33*, 3. [[CrossRef](#)]
14. Bian, J.W.; Fall, M.; Haruna, S. Sulfate-induced changes in rheological properties of fibre-reinforced cemented paste backfill. *Mag. Concr. Res.* **2021**, *73*, 574–583. [[CrossRef](#)]
15. Roshani, A.; Fall, M. Rheological properties of cemented paste backfill with nano-silica: Link to curing temperature. *Ement Concr. Compos.* **2020**, *144*. [[CrossRef](#)]
16. Xue, Z.L.; Gan, D.Q.; Zhang, Y.Z. Rheological behavior of ultrafine-tailings cemented paste backfill in high-temperature mining conditions. *Constr. Build. Mater.* **2020**, *253*, 119212. [[CrossRef](#)]

17. Ouattara, D.; Yahia, A.; Mbonimpa, M.; Belem, T. Effects of superplasticizer on rheological properties of cemented paste backfills. *Int. J. Miner. Process.* **2017**, *161*, 28–40. [[CrossRef](#)]
18. Fall, M.; Célestin, J.C.; Pokharel, M.; Touré, M. A contribution to understanding the effects of curing temperature on the mechanical properties of mine cemented tailings backfill. *Eng. Geol.* **2010**, *114*, 397–413. [[CrossRef](#)]
19. Zhang, S.Y.; Yang, L.; Ren, F.Y. Rheological and mechanical properties of cemented foam backfill: Effect of mineral admixture type and dosage. *Cem. Concr. Comp.* **2020**, *112*, 103689. [[CrossRef](#)]
20. Guo, Z.B.; Qiu, J.P.; Jiang, H.Q. Flowability of ultrafine-tailings cemented paste backfill incorporating superplasticizer: Insight from water film thickness theory. *Powder Technol.* **2021**, *381*, 509–517. [[CrossRef](#)]
21. Majid, U.; Mohammad, N.; Seiyd, Z.S. Modeling the effects of ore properties on water recovery in the thickening process. *Int. J. Min. Met. Mater.* **2014**, *21*, 851–861. [[CrossRef](#)]
22. Lima, P.; Gomes, O.; Filho, R.D.T. Influence of Recycled Aggregate on the Rheological Behavior of Cement Mortar. *Key Eng. Mater.* **2014**, *600*, 297–307. [[CrossRef](#)]
23. Jiao, D.W.; Shi, C.J.; Yuan, C.Q. Influences of shear-mixing rate and fly ash on rheological behavior of cement pastes under continuous mixing. *Constr. Build. Mater.* **2018**, *188*, 170–177. [[CrossRef](#)]
24. Ouattara, D.; Mbonimpa, M.; Yahia, A.; Belem, T. Assessment of rheological parameters of high density cemented paste backfill mixtures incorporating superplasticizers. *Constr. Build. Mater.* **2018**, *190*, 294–307. [[CrossRef](#)]
25. Ke, X.; Hou, H.; Zhou, M.; Wang, Y.; Zhou, X. Effect of particle gradation on properties of fresh and hardened cemented paste backfill. *Constr. Build. Mater.* **2015**, *96*, 378–382. [[CrossRef](#)]
26. Deng, X.J.; Klein, B.; Tong, L.; de Wit, B. Experimental study on the rheological behavior of ultra-fine cemented backfill. *Constr. Build. Mater.* **2018**, *158*, 985–994. [[CrossRef](#)]
27. Deng, X.J.; Klein, B.; Hallbom, D.J.; de Wit, B.; Zhang, J.X. Influence of particle size on the basic and time-dependent rheological behaviors of cemented paste backfill. *J. Mater. Eng. Perform.* **2018**, *27*, 3478–3487. [[CrossRef](#)]
28. Xu, W.B.; Tian, M.M.; Li, Q.L. Time-dependent rheological properties and mechanical performance of fresh cemented tailings backfill containing flocculants. *Miner. Eng.* **2020**, *145*, 106064. [[CrossRef](#)]
29. Peng, X.P.; Fall, M.; Haruna, S. Sulphate induced changes of rheological properties of cemented paste backfill. *Miner. Eng.* **2019**, *141*, 105849. [[CrossRef](#)]
30. Zhao, Y.; Taheri, A.; Karakus, M. Effects of water content, water type and temperature on the rheological behaviour of slag-cement and fly ash-cement paste backfill. *Int. J. Min. Sci. Techno.* **2020**, *30*, 271–278. [[CrossRef](#)]
31. Ruiz-Hernando, M.; Labanda, J.; Llorens, J. Effect of ultrasonic waves on the rheological features of secondary sludge. *Biochem. Eng. J.* **2010**, *52*, 131–136. [[CrossRef](#)]
32. Luo, X.M.; Gong, H.Y.; He, Z.L. Research on mechanism and characteristics of oil recovery from oily sludge in ultrasonic fields. *J. Hazard. Mater.* **2020**, *399*, 123137. [[CrossRef](#)]
33. Wang, K.Z.; Lv, W.S.; Yang, P. Effect of ultrasonic waves on rheological properties of backfilling slurry and prediction of rheological parameters. *T. Nonferr. Metal. Soc.* **2018**, *28*, 1442–1451. [[CrossRef](#)]
34. Zhu, L.Y.; Lv, W.S.; Yang, P. Effect of Ultrasonic on Rheological Properties of Unclassified Tailings Slurry. *Mater. Rep.* **2020**, *34*, 06088–06094. [[CrossRef](#)]
35. Jiao, H.Z.; Wang, S.F.; Yang, Y.X. Water recovery improvement by shearing of gravity-thickened tailings for cemented paste backfill. *J. Clean. Prod.* **2020**, *245*, 118882. [[CrossRef](#)]
36. Sivakugan, N.; Veenstra, R.; Naguleswaran, N. Underground mine backfilling in ustralia using aste fills and hydraulic fills. *Int. J. Geosynth. Ground Eng.* **2015**, *18*, 1. [[CrossRef](#)]
37. Lee, J.K.; Ko, J.; Kim, Y.S. Rheology of fly ash mixed tailings slurries and applicability of rediction models. *Minerals* **2017**, *9*, 165. [[CrossRef](#)]
38. Paterson, A.J.C. Pipeline transport of high density slurries: A historical review of past mistakes, lessons learned and current technologies. *Min. Technol. Trans. Inst. Min. Metall.* **2012**, *121*, 37–45. [[CrossRef](#)]
39. Panchal, S.; Deb, D.; Sreenivas, T. Variability in rheology of cemented paste backfill with hydration age, binder and superplasticizer dosages. *Adv. Powder Technol.* **2018**, *29*, 2211–2220. [[CrossRef](#)]
40. Smythe, M.C.; Wakeman, R.J. The use of acoustic fields as a filtration and dewatering aid. *Ultrasonics* **2000**, *38*, 657–661. [[CrossRef](#)]
41. Hawkes, J.J.; Limaye, M.S.; Coakley, W.T. Filtration of bacteria and yeast by ultrasound-enhanced sedimentation. *J. Appl. Microbiol.* **1997**, *82*, 39–47. [[CrossRef](#)] [[PubMed](#)]